A Water-Stable Zinc(II)-Organic Framework as a Multiresponsive Luminescent Sensor for Toxic Heavy Metal Cations, Oxyanions and Organochlorine Pesticides in Aqueous Solution

Xiao-Qing Wang*[a], Dou-Dou Feng[a], Jing Tang[a], Yu-Di Zhao[a], Jun Li[a], Jie Yang[b], Chan Kyung Kim[c]*, Feng Su*[d]

a. *North University of China, Tai Yuan, P. R. China. E-mail; xqwang@nuc.edu.cn*;

b. *Liaocheng University, Liaocheng, P. R. China;*

c. Department of Chemistry and Chemical Engineering, Inha University, Incheon 22212, Korea. *E-mail; kckyung@inha.ac.kr*;

d. Department of Chemistry, Changzhi University, Changzhi 046011, China.

1. Photoluminescent sensing experiments.

The luminescence properties of complex **1** have been researched in the solid state and various analytes at room temperature. For sensing of cations and anions, 2.0 mg of a powder sample of complex **1** was dispersed in aqueous solution (2.0 ml) of $M(NO_3)_x$ (M^{x+} =Hg^{2+}, Zn^{2+}, Ag^{+}, Na^{+}, Ni^{2+}, Co^{2+}, Ca^{2+}, Ba^{2+}, Mn^{2+}, Mg^{2+}, Cd^{2+}, Fe^{2+}, Al^{3+}, Cr^{3+} and Fe^{3+}, 0.010 mol•L^{-1}) or K_yX (X = Br^{-}, SO_4^{2-}, NO_3^{-}, SCN^{-}, Cl^{-}, CH_3COO^{-}, HCO_3^{-}, I^{-}, $C_2O_4^{2-}$, CO_3^{2-}, HPO_4^{2-}, $H_2PO_4^{-}$ PO_4^{3-}, CrO_4^{2-}, $Cr_2O_7^{2-}$ and MnO_4^{-}). For sensing of 2,6-Dich-4-NA, a diluent pesticide solution (in acetonitrile solvent) was added in the suspension of complex **1** (in water solvent), then the luminescence property was investigated. Several pesticides were selected including carbaryl, chlorobenzene (CB), atrazine, 2,4-dichlorobenzene (2,4-DCP), 1,2-dichlorobenzene (1,2-DiCB), 1,2,4-trichlorobenzene (1,2,4-TriCB), 1,2,4,5-tetrachlorobenzene (1,2,4,5-TetraCB) and 2,6-dichloro-4-nitroamine (2,6-Dich-4-NA).

2. Fluorescence Titration experiments.

The 2.0 mg powder sample of complex **1** was dispersed in 2.0 mL solution of target analytes with different concentrations.

3. Time-dependent fluorescence sensing experiments.

The fluorescence intensities of complex **1** within the Cr^{3+} solution (1.5 mM), Fe^{3+} solution (0.55 mM), $Cr_2O_7^{2-}$ solution (1.3 mM), MnO_4^{-} solution (1.0 mM) and 2,6-Dich-4-NA solution (0.4 mM) were recorded at 30 s, 1 min, 2 min, 3 min, 4 min, 5 min and 6 min.

4. **Fluorescence recognition experiments at different pH values.**

0.01 mM Cr^{3+}, Fe^{3+} CrO_4^{2-} and MnO_4^- aqueous solutions with pH of 2 and 10 were configured respectively. A powder sample of complex **1** (2.0 mg) was dispersed in these aqueous solution (2.0 ml), and the fluorescence emission spectrum of the complex **1** was recorded.

5. Recyclable Luminescence Experiments.

The powder of complex **1** was centrifuged from the suspension and rinsed with distilled water for three times. Then, the recovered sample was dried and added to the target analytes again to measure their emission spectra. The same procedure was repeated five times.

6. Sensing of 2,6-Dich-4-NA in practical samples.

For sensing 2,6-Dich-4-NA in sodium dodecyl sulfate (SDS): In the presence of SDS, 2,6-Dich-4-NA pesticide was gradually added to the cuvette and the corresponding fluorescence emission spectra were recorded.

For sensing 2,6-Dich-4-NA in carrot, nectarine and grape extracts: 50 mg solid mass of a carrot (finely chopped) without peal is taken in a 250 mL clean beaker, then 60 ml distilled water was add and lightly mixed again. Next, the mixture was heated to 50 ℃ and stirred continuously for two hours on a magnetic stirrer. The mixture was cooled down to ambient temperature and collected liquid through filter paper. The filtrate was centrifuged at 2000 rpm for 30 min. When all of that is done, the supernatant was collected for luminescence study. The procedure was the same as that for carrot extract, except that nectarine, grape were replaced by carrot.[1] 100 μL of carrot extract was added into the solution of 2 $mg \cdot mL^{-1}$ complex **1**, and a stable suspension was obtained after 30 min of ultrasound. Then, acetonitrile solution of 2,6-Dich-4-NA was added into the suspension step by step, and the fluorescence emission spectrum of the complex **1** was recorded.

Table S1 Selected bond lengths (Å) and angles (°) for complex **1**.

Zn1—O11	2.143 (6)	Zn1—N2	2.100 (7)
Zn1—O1	2.100 (7)	Zn2—O11	1.999 (6)
Zn1—O4	2.064 (6)	Zn2—O9	2.110 (6)
Zn1—O10	2.095 (6)	Zn2—O3	1.970 (6)
Zn1—O8	2.198 (6)	Zn1—N2	2.100 (7)
Zn2—N1	2.029 (7)	O2—Zn3^{iii}	1.949 (6)
Zn2—O5	2.310 (6)	C17—C22^{i}	1.508 (12)
Zn3—O7	1.975 (6)	C20—C10^{ii}	1.497 (11)

Zn3—O11	1.959 (6)	C23—C12^{iv}	1.511 (11)
Zn3—O6	1.977 (7)	C4—C21^{v}	1.507 (12)
C1—O2—Zn3^{iii}	118.9 (6)	O4—Zn1—O1	172.1 (3)
O11—Zn1—O8	88.2 (2)	O4—Zn1—O10	87.0 (2)
O1—Zn1—O11	83.2 (2)	O4—Zn1—O8	96.3 (2)
O1—Zn1—O8	89.3 (3)	O4—Zn1—N2	92.5 (3)
O4—Zn1—O11	91.3 (2)	O10—Zn1—O11	97.3 (2)
O10—Zn1—O1	87.9 (3)	N2—Zn1—O8	83.2 (3)
O10—Zn1—O8	173.5 (2)	O11—Zn2—O9	92.6 (3)
O10—Zn1—N2	91.1 (3)	O11—Zn2—N1	112.3 (3)
N2—Zn1—O11	171.0 (3)	O11—Zn2—O5	90.9 (2)
N2—Zn1—O1	93.7 (3)	O9—Zn2—O5	173.8 (2)
O3—Zn2—O11	126.1 (2)	O11—Zn3—O7	114.2 (2)
O3—Zn2—O9	90.8 (2)	O11—Zn3—O6	105.0 (3)
O3—Zn2—N1	120.8 (3)	C22—O7—Zn3	106.6 (5)
O3—Zn2—O5	83.1 (2)	Zn2—O11—Zn1	99.9 (3)
N1—Zn2—O9	95.4 (3)	Zn3—O11—Zn1	109.0 (3)
N1—Zn2—O5	87.9 (3)	Zn3—O11—Zn2	116.0 (3)
O2^{iii}—Zn3—O7	113.1 (3)	C1—O1—Zn1	151.7 (6)
O2^{iii}—Zn3—O11	120.2 (3)	C14—O4—Zn1	133.3 (6)
O2^{iii}—Zn3—O6	96.6 (3)	C23—O10—Zn1	132.5 (5)
O7—Zn3—O6	104.2 (2)	C33—N2—Zn1	C33—N2—Zn1

Symmetry codes: (i) −x+1/2, y−1/2, −z+1/2; (ii) x+1/2, −y+1/2, z+1/2; (iii) −x+1/2, −y+1/2, −z; (iv) −x, −y, −z; (v) x−1/2, −y+1/2, z−1/2; (vi) x+1/2, y−1/2, z; (vii) −x+1/2, y+1/2, −z+1/2; (viii) x−1/2, y+1/2, z.

Table S2. Hydrogen bonding geometry (Å, º) for complex **1**.

D – H ⋯ A	**D – H / Å**	**H ⋯A / Å**	**D ⋯ A / Å**	**D – H ⋯A / °**
O11-H11...O7^{iii}	0.85	2.03	2.8694(3)	174

O12-H12A...O3^{vii}	0.85	2.28	3.0143(3)	145
O12-H12B...O5^{vii}	0.85	2.28	3.0224(3)	146

Symmetry code: (iii) −x+1/2, −y+1/2, −z; (vii) −x+1/2, y+1/2, −z+1/2.

Table S3. Performance of reported MOFs for detecting Cr(Ⅲ).

	MOF	K_{sv}(M^{-1})	Detection Limit	Medium Used	Ref.
1	[Zn(DDB)(DPE)]·H_2O	7.6×10^4	1.2×10^{-7} M	H_2O	This work
2	[Eu(L)(HCOO)(H_2O)]$_n$	1356.9	1.5 μmol L^{-1}	H_2O	5e
3	[Tb(L)(HCOO)(H_2O)]$_n$	999.5	1.9 μmol L^{-1}	H_2O	5e
4	{[Zn_2(m_3-OH)(cpta)(4,4′-bipy)]·H_2O}$_n$	9.47×10^3	5.55×10^{-6} M	H_2O	26a
5	[Zn_2(TPOM)(NH_2–BDC)$_2$]·$4H_2O$	-	4.9 mM	H_2O	5c
6	{[Zn_2(tpeb)$_2$(2,3-ndc)$_2$]·H_2O}$_n$	50972	2.87×10^{-7} M	H_2O	5a
7	{[Eu_3(bpydb)$_3$(HCOO)$(OH)_2$-(DMF)]·3DMF·$2H_2O$}$_n$	2.24×10^3	1.0×10^{-6} M	H_2O	26b
8	[Eu_2(tpbpc)$_4$·CO_3·$4H_2O$]·DMF·solvent	5.14×10^2	3.64 ppm	H_2O	5b
9	Me_2NH_2]$_4$[Zn_6(qptc)$_3$(trz)$_4$]·$6H_2O$	4.39×10^4	1 μmol/L	H_2O	26c

Table S4. Performance of reported MOFs for detecting Fe(Ⅲ).

	MOF	$K_{sv}(M^{-1})$	Detection Limit	Medium Used	Ref.
1	$[Zn(DDB)(DPE)]\cdot H_2O$	1.4×10^4	1.8×10^{-7}M	H_2O	This work
2	$\{[Cd(L)(H_2O)_2]\cdot4H_2O\}_n$	7.2×10^4	0.78μM	H_2O	27(a)
3	$[TbL\cdot2H_2O)]_n$	2.27×10^4	8.32×10^{-6}M	H_2O	27(b)
4	$\{[Eu_2(L)_2(H_2O)_2]\cdot5H_2O\cdot6DMAC\}_n$	5941	10^{-5}M	H_2O	27(c)
5	$\{Zn_2(tpt)_2(tad)_2\cdot H_2O\}$	4.72×10^4	4.72×10^{-6}M	H_2O	27(d)
6	$Ti_2(HDOBDC)_2(H_2DOBDC)$	-	0.45μM	H_2O	27(e)
7	$[(CH_3)_2NH_2]\cdot[Tb(bptc)]\cdot$xsolvents	0.1801mM		H_2O	27(f)
8	$\{[Cd_2(L)(DMA)]\cdot H_2N(Me)_2\}_n$	4.9×10^3	1.2×10^{-3}M	H_2O	27(g)
9	$\{Zn_2(NO_3)_2(4,4'\text{-bpy})_2(TBA)\}$	-	1.2×10^{-6}M	H_2O	27(h)
10	$[CH_3\text{-dpb}]_2[Mg_3(1,4\text{-NDC})_4(\mu\text{-}H_2O)_2(CH_3OH)(H_2O)]\cdot1.5H_2O$	0.16×10^5	4.7×10^{-4}M	H_2O	27(i)

Table S5. Performance of reported MOFs for detecting CrO_4^{2-}.

	MOF	$K_{sv}(M^{-1})$	Detection Limit	Medium Used	Ref.
1	$[Zn(DDB)(DPE)]\cdot H_2O$	1.4×10^4	6.4×10^{-7} M	H_2O	This work
2	$[Eu(L)(HCOO)(H_2O)]_n$	1537.4	1.2 μmol L^{-1}	H_2O	5e
3	$[Tb(L)(HCOO)(H_2O)]_n$	1307.0	1.8 μmol L^{-1}	H_2O	5e

4	$[Zn_2(TPOM)(NH_2–BDC)_2]\cdot 4H_2O$	4.45×10^3	4.8 μM	H_2O	5c
5	$\{[Zn_2(tpeb)_2(2,3\text{-}ndc)_2]\cdot H_2O\}_n$	73481	1.734 ppb	H_2O	5a
6	$[Eu_2(tpbpc)_4\cdot CO_3\cdot 4H_2O]\cdot DMF\cdot solvent$	4.85×10^3	0.33 ppm	H_2O	5b
7	$[Zn(L)(bpeb)](DMAC)_{2.5}$	0.82×10^4	4.4×10^{-5} M	H_2O	28a
8	$\{[La(SIP)(H_2O)_3]\cdot H_2O\}_n$	6.722×10^3	-	H_2O	28b

Table S6. Performance of reported MOFs for detecting $Cr_2O_7^{2-}$.

	MOF	$K_{sv}(M^{-1})$	Detection Limit	Medium Used	Ref.
1	$[Zn(DDB)(DPE)]\cdot H_2O$	1.4×10^4	6.4×10^{-7} M	H_2O	This work
2	$[Eu(L)(HCOO)(H_2O)]_n$	2762.6	1.0μmol·L^{-1}	H_2O	5e
3	$[Tb(L)(HCOO)(H_2O)]_n$	2133.5	2.1μmol·L^{-1}	H_2O	5e
4	$\{[Zn_2(\mu_3\text{-}OH)(cpta)(4,4'\text{-}bipy)]\cdot H_2O\}_n$	5.45×10^3	$6.91\cdot10^{-6}$ M	H_2O	26a
5	$[Zn(ACA)_4]\cdot CB[6]\cdot[NH_2(CH_3)_2]\cdot 8H_2O$	6.0×10^3	3.9×10^{-6} M	H_2O	28c
6	$[Zn_2(TPOM)(NH_2–BDC)_2]\cdot 4H_2O$	7.59×10^3	3.9 μM	H_2O	5c
7	$\{[Zn_2(tpeb)_2(2,3\text{-}ndc)_2]\cdot H_2O\}_n$	70913	2.623 ppb	H_2O	5a
8	$[Zr_6O_4(OH)_8(H_2O)_4(TCPP)_4]\cdot 9DMF\cdot 3.5H_2O$	5.91×10^4	0.38 μM	H_2O	28d
9	$\{[Eu_3(bpydb)_3(HCOO)(OH)_2\text{-}(DMF)]\cdot 3DMF\cdot 2H_2O\}_n$	1.33×10^4	5.0×10^{-7} M	H_2O	26b
10	$[Eu_2(tpbpc)_4\cdot CO_3\cdot 4H_2O]\cdot DMF\cdot solvent$	1.04×10^4	1.07 ppm	H_2O	5b
11	$[Zn(L)(bpeb)](DMAC)_{2.5}$	2.27×10^4	1.6×10^{-5} M	H_2O	28a
12	$\{[La(SIP)(H_2O)_3]\cdot H_2O\}_n$	1.580×10^4	-	H_2O	28b

Table S7. Performance of reported MOFs for detecting MnO_4^-

	MOF	$K_{sv}(M^{-1})$	Detection Limit	Medium Used	Ref.
1	$[Zn(DDB)(DPE)]\cdot H_2O$	3.4×10^4	2.7×10^{-7}M	H_2O	This work
2	$[Pb_3(BPDP)_{1.5}(OOCC_6H_4COOH)_3]$	1.1×10^4	-	H_2O	29(a)
3	$\{[Eu(bpydb)_3(HCOO)(OH)_2(DMF)]3DMF\cdot2H_2O\}_n$	2.45×10^4	1.0×10^{-7}M	H_2O	23(b)
4	$[Cd(L)_2(H_2O)_2]_n$	2.2×10^4	1.73×10^{-4}M	H_2O	29(b)
5	$\{[Eu_2(L)_2(H_2O)_2]\cdot5H_2O\cdot6DMAC\}_n$	1200	4.48×10^{-5}M	H_2O	27(c)
6	CDs@MOF(Eu)	3.64×10^4	6.8×10^{-5}M	H_2O	29(c)
7	534-MOF-Tb	6.63×10^4	3.4×10^{-4}M	H_2O	29(d)
8	$\{[Zn_3(L)(OH)(H_2O)_5]\cdot NMP\cdot2H_2O\}_n$	1.1×10^4	1.81×10^{-3}M	H_2O	29(e)
9	$\{[Ba_3La_{0.5}(\mu_3\text{-}L)_{2.5}(H_2O)_3(DMF)]\cdot(3DMF)\}_n(1.3DMF)$	7.73×10^4	0.28μM	H_2O	29(f)
10	$\{[Eu_2Na(Hpddb)(pddb)_2(CH_3COO)_2]\cdot2.5(DMA)\}_n$	2.84×10^3	5.99μM	H_2O	29(g)

Table S8. Performance of reported MOFs for detecting 2,6-Dich-4-NA.

	MOF	$K_{sv}(M^{-1})$	Detection Limit	Medium Used	Ref.
1	$[Zn(DDB)(DPE)]\cdot H_2O$	3.3×10^4	166 ppb	H_2O	This work
2	$[Ag(CIP^-)]$	5.2×10^4	105 ppb	DMF	17e
3	$[Mg_2(APDA)_2(H_2O)_3]\cdot5DMA\cdot5H_2O$	7.5×10^4	150 ppb	DMF	17d
4	$[Zn_2(bpdc)_2(BPyTPE)]$	-	0.13 ppm	DCM	12
5	$[Zn_2(L)_2(TPA)]_2H_2O$	2.36×10^4	0.39 ppm	Methanol	17a

6	$[Cd_3(CBCD)_2(DMA)_4(H_2O)_2]\cdot 10DMA$	4.47×10^4	145 ppb	DMA	30

Table S9. HOMO and LUMO energy levels of H_5DDB and 8 pesticides. Optical gap calculation using DFT [Basis set B3LYP/6-31G(d) using Gaussian 16]

GAS	B3LYP/6-31G(d)	HOMO(H)	LUMO(H)	HOMO(eV)	LUMO(eV)	ΔE(eV)
H_5DDB	-1637.206931	-0.2427	-0.07314	-6.60	-1.99	4.61
2,6-Dich-4-NA	-1411.296332	-0.24319	-0.08841	-6.62	-2.41	4.21
Carbaryl	-669.126791	-0.20794	-0.03539	-5.66	-0.96	4.70
CB	-691.844975	-0.24641	-0.01255	-6.71	-0.34	6.36
Atrazine	-1047.283122	-0.23561	-0.01483	-6.41	-0.40	6.01
2,4-DCP	-1226.657223	-0.23931	-0.02669	-6.51	-0.73	5.79
1,2-DiCB	-1151.435734	-0.25151	-0.02413	-6.84	-0.66	6.19
1,2,4-TriCB	-1611.0292	-0.25446	-0.03761	-6.92	-1.02	5.90
1,2,4,5-TetraCB	-2070.617986	-0.25805	-0.04746	-7.02	-1.29	5.73

Table S10. HOMO and LUMO energy levels of H_5DDB and 8 pesticides. Optical gap calculation using DFT [Basis set B3LYP/6-311G+(d,p) using Gaussian 16]

GAS	B3LYP/6-311+G(d,p)	HOMO(H)	LUMO(H)	HOMO(eV)	LUMO(eV)	ΔE(eV)
H_5DDB	-1637.696816	-0.25991	-0.0883	-7.07	-2.40	4.67
2,6-Dich-4-NA	-1411.497444	-0.25533	-0.10528	-6.95	-2.86	4.08
Carbaryl	-669.3097468	-0.22234	-0.05245	-6.05	-1.43	4.62
CB	-691.9342149	-0.2575	-0.03171	-7.01	-0.86	6.14
Atrazine	-1047.476614	-0.24783	-0.02882	-6.74	-0.78	5.96
2,4-DCP	-1226.804061	-0.25126	-0.04391	-6.84	-1.19	5.64
1,2-DiCB	-1151.551819	-0.26131	-0.04161	-7.11	-1.13	5.98
1,2,4-TriCB	-1611.17225	-0.26276	-0.05346	-7.15	-1.45	5.70
1,2,4,5-TetraCB	-2070.78803	-0.26544	-0.06221	-7.22	-1.69	5.53

Table S11. HOMO and LUMO energy levels of H_5DDB and 8 pesticides. Optical gap calculation using PCM-DFT in aqueous solution [Basis set B3LYP/6-311+G(d,P) using Gaussian 16]

H_2O	B3LYP/6-311+G(d,p)	HOMO(H)	LUMO(H)	HOMO(eV)	LUMO(eV)	ΔE(eV)
H_5DDB	-1637.727644	-0.26072	-0.0886	-7.09	-2.41	4.68
2,6-Dich-4-NA	-1411.508404	-0.24506	-0.11062	-6.67	-3.01	3.66
Carbaryl	-669.3225626	-0.2323	-0.06028	-6.32	-1.64	4.68
CB	-691.937562	-0.26011	-0.03162	-7.08	-0.86	6.22
Atrazine	-1047.486791	-0.25373	-0.03671	-6.90	-1.00	5.91
2,4-DCP	-1226.808827	-0.24963	-0.04159	-6.79	-1.13	5.66
1,2-DiCB	-1151.555542	-0.26286	-0.03941	-7.15	-1.07	6.08
1,2,4-TriCB	-1611.175652	-0.2614	-0.04873	-7.11	-1.33	5.79
1,2,4,5-TetraCB	-2070.791138	-0.26256	-0.05603	-7.14	-1.52	5.62

Table S12. HOMO and LUMO energy levels of H_5DDB and 8 pesticides. Optical gap calculation using PCM-DFT [Basis set cam-B3LYP/6-311+G(d,p) using Gaussian 16].

GAS	cam-B3LYP/6-311+G(d,p)	HOMO(H)	LUMO(H)	HOMO(eV)	LUMO(eV)	ΔE(eV)
H_5DDB	-1636.984232	-0.30979	-0.04098	-8.43	-1.12	7.31
2,6-Dich-4-NA	-1411.275568	-0.30441	-0.05696	-8.28	-1.55	6.73
Carbaryl	-668.9709845	-0.27107	-0.00776	-7.38	-0.21	7.17
CB	-691.793823	-0.31012	0.01546	-8.44	0.42	8.86
Atrazine	-1047.177689	-0.30274	0.01989	-8.24	0.54	8.78
2,4-DCP	-1226.647904	-0.30328	0.002	-8.25	0.05	8.31
1,2-DiCB	-1151.415098	-0.31377	0.005	-8.54	0.14	8.67
1,2,4-TriCB	-1611.038994	-0.31472	-0.00704	-8.56	-0.19	8.37
1,2,4,5-TetraCB	-2070.658401	-0.31717	-0.01633	-8.63	-0.44	8.19

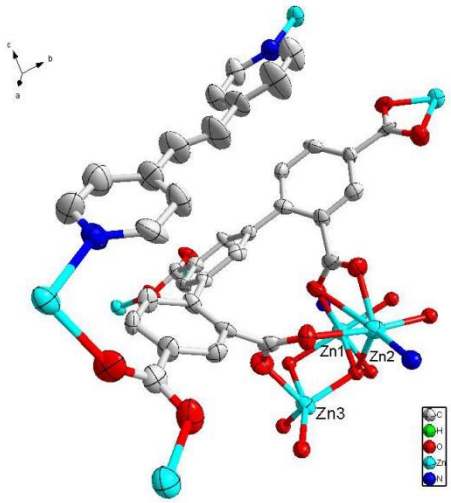

Fig. S1 Coordination environment of Zn(Ⅱ) ion in complex **1**.

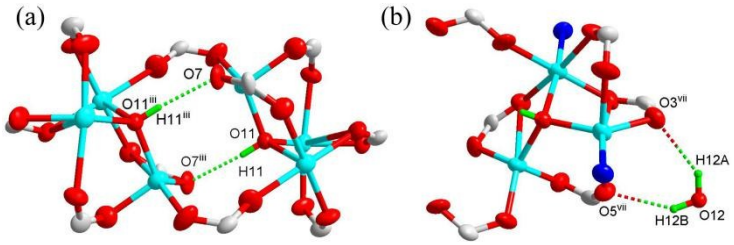

Fig. S2 The intramolecular hydrogen bonds of complex **1**. Symmetry code: (iii) −x+1/2, −y+1/2, −z; (vii) −x+1/2, y+1/2, −z+1/2.

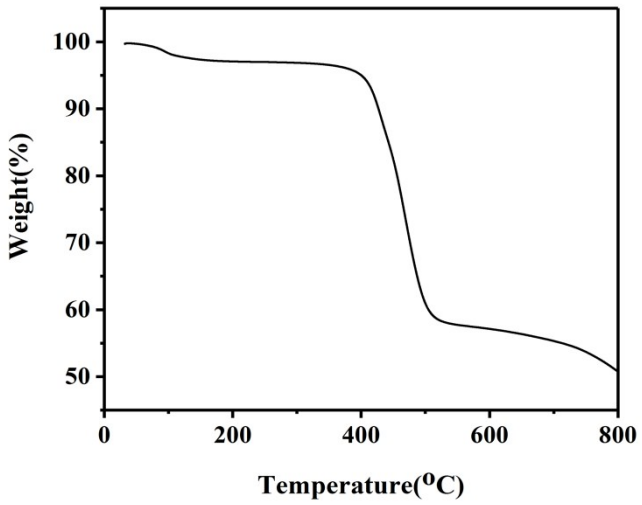

Fig. S3 The TGA curves of complex **1**.

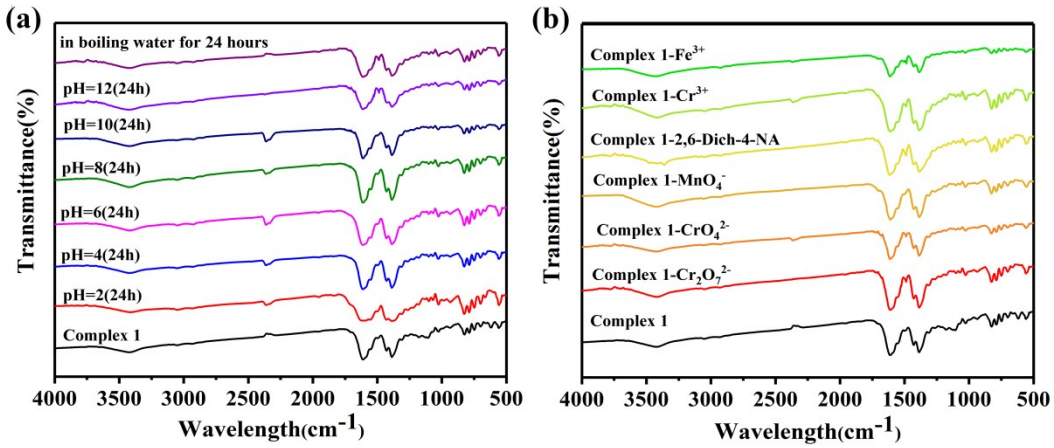

Fig. S4 (a) FTIR of complex **1** after immersed in boiling water for 24 h and in acidic and basic aqueous solution using an extensive pH range of 2-12 for 24 h. (b) FTIR of complex **1** before and after exposure to different analytes.

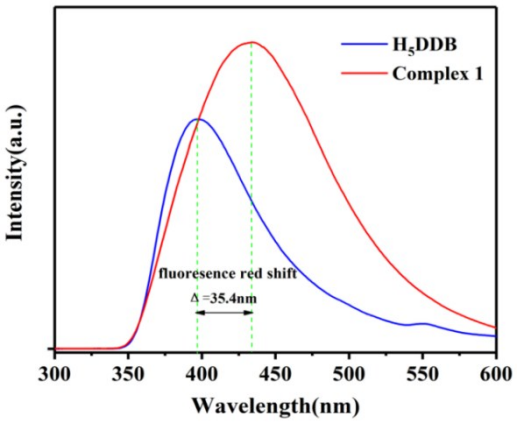

Fig. S5 Solid-state luminescence spectra of the H_5DDB ligand and complex **1**.

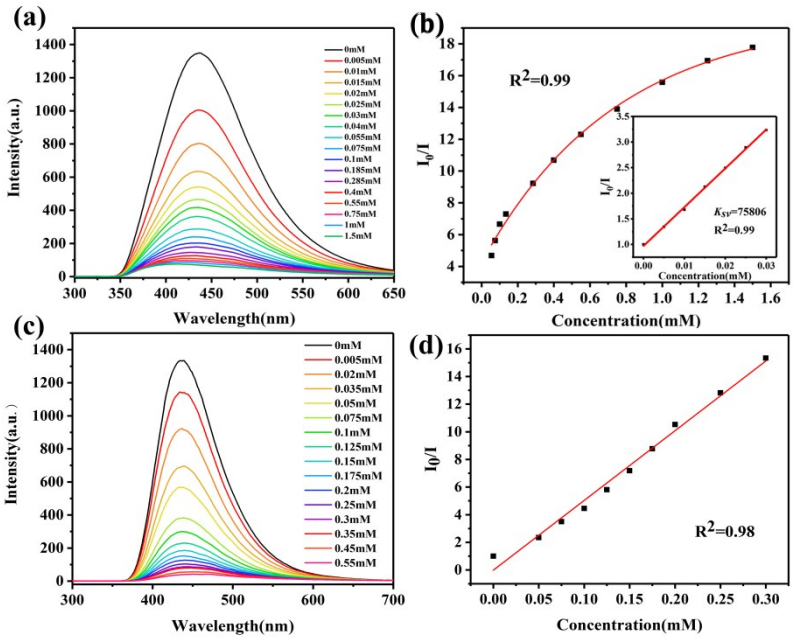

Fig. S6 The fluorescence spectra of complex **1** with different concentrations of Cr^{3+} (a) and Fe^{3+} (e) in aqueous solution; SV plot of complex **1** for sensing of Cr^{3+} (b) and Fe^{3+} (d); in aqueous solution. Inset: linear fitting part.

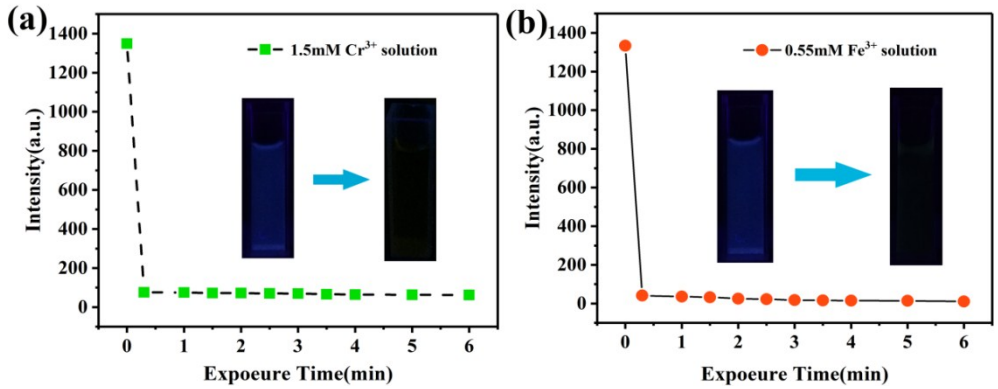

Fig. S7 (a)The fluorescence intensity of complex **1** in Cr^{3+} solution as a function of exposure time. Inset : the color changes of complex **1** induced by the addition of 1.5 mM Cr^{3+} ions under 365 nm UV light; (b)The fluorescence intensity of complex **1** in Fe^{3+} solution as a function of exposure time. Inset : the color changes of complex **1** induced by the addition of 0.55 mM Fe^{3+} ions under 365 nm UV light.

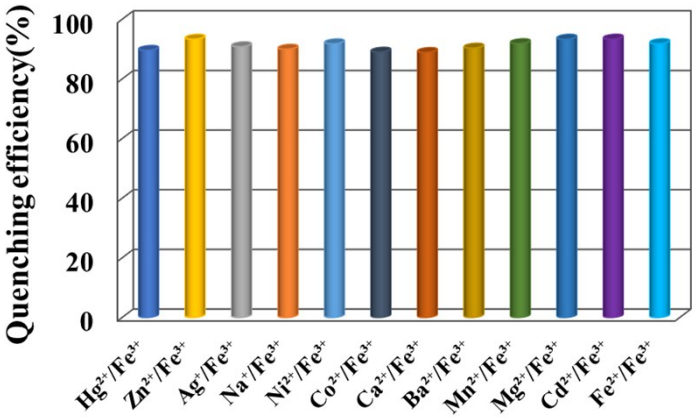

Fig. S8 The effect of other metal cations on the quenching efficiency of Fe^{3+}.

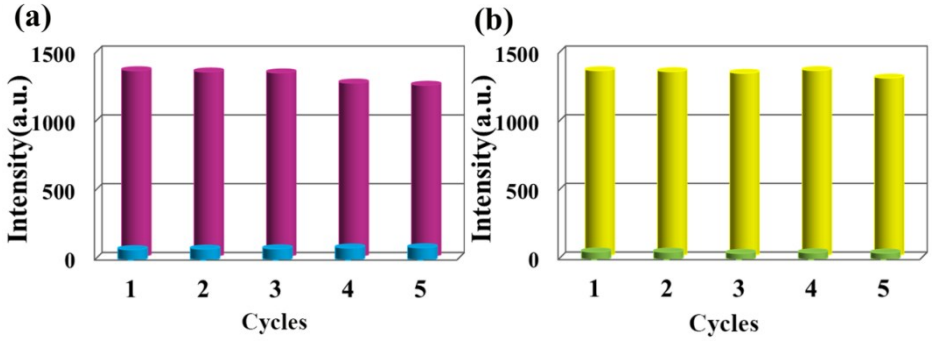

Fig. S9 (a) The cyclic response of the luminescence intensities of complex **1** for detecting Cr^{3+}; (b) The cyclic response of the luminescence intensities of complex **1** for detecting Fe^{3+}.

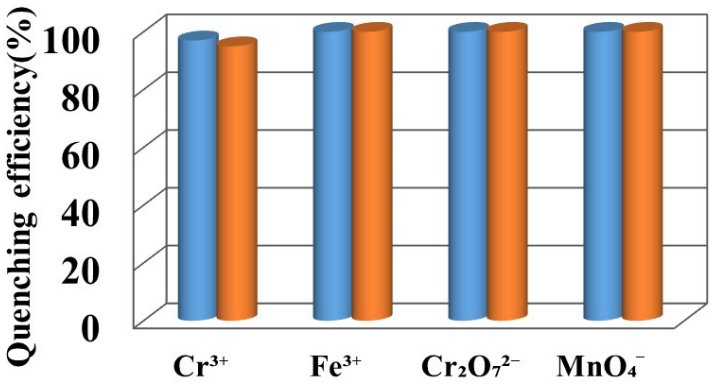

Fig. S10 Fluorescence recognition experiments at different pH values. Blue columns stand for the luminescence intensities of complex **1** in an acid (pH=2) aqueous solution. Yellow columns stand for the luminescence intensities of complex **1** in a base (pH=10) aqueous solution.

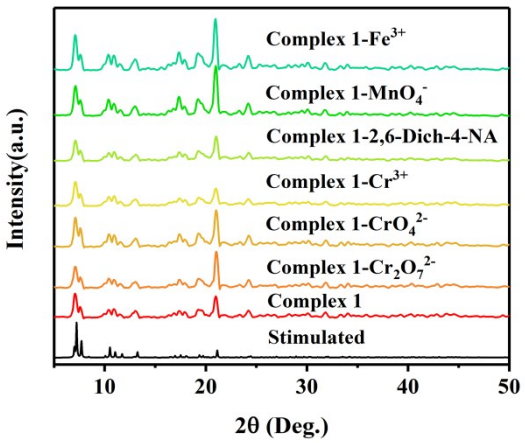

Fig. S11 PXRD patterns of complex **1** before and after exposure to different analytes.

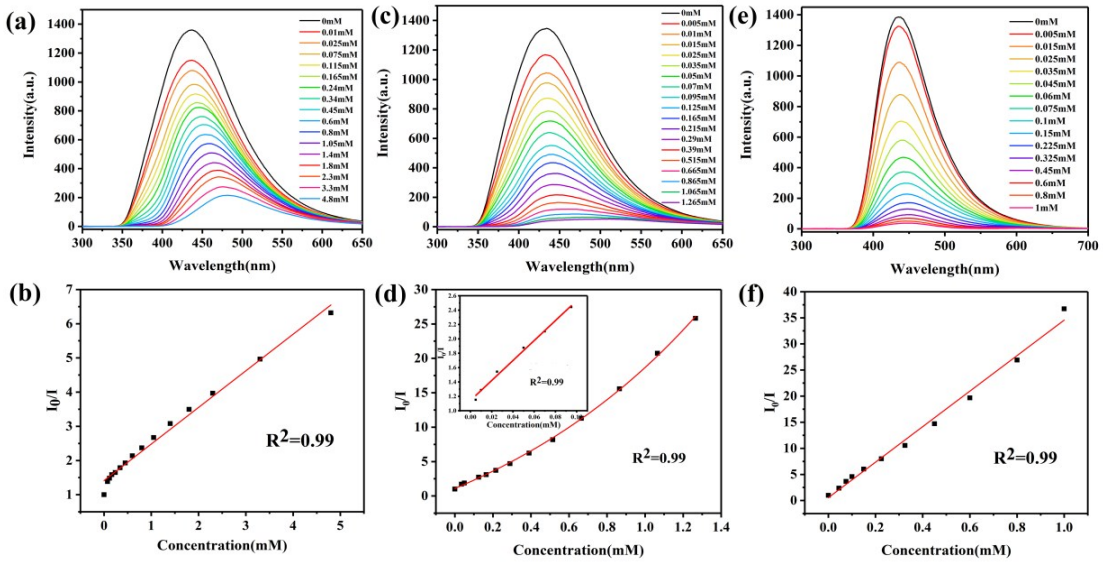

Fig. S12 The fluorescence spectra of complex **1** with different concentrations of CrO_4^{2-} (a), $Cr_2O_7^{2-}$ (c) and MnO_4^- (e) in aqueous solution; SV plot of complex **1** for sensing of CrO_4^{2-} (b), $Cr_2O_7^{2-}$ (d) and MnO_4^- (f) in aqueous solution. Inset: linear fitting part.

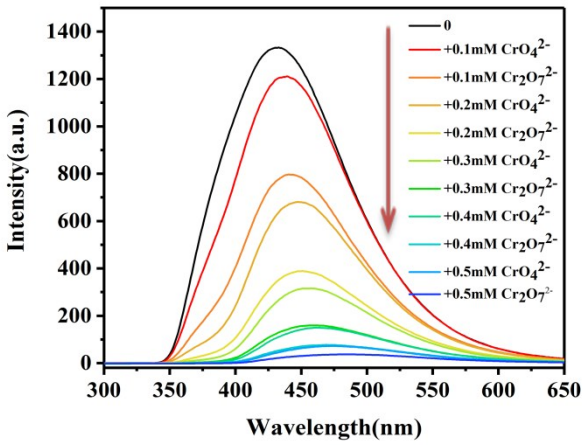

Fig. S13 Fluorescence spectra of competitive quenching of CrO_4^{2-} and $Cr_2O_7^{2-}$.

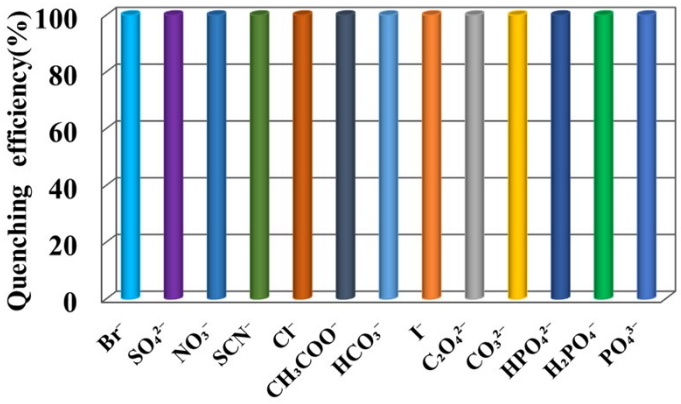

Fig. S14 The effect of other anions on the quenching efficiency of MnO_4^-.

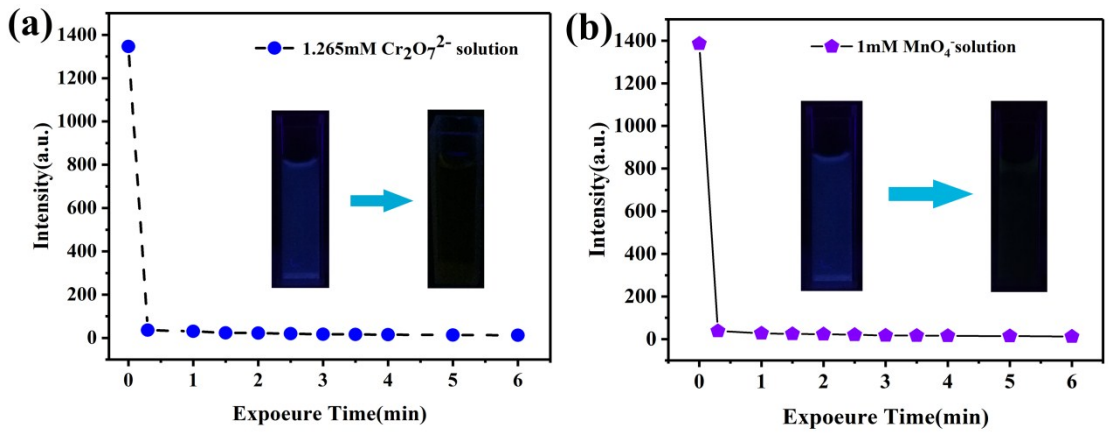

Fig. S15 (a) The fluorescence intensity of complex **1** in $Cr_2O_7^{2-}$ solution as a function of exposure time. Inset : the color changes of complex **1** induced by the addition of 1.27 mM $Cr_2O_7^{2-}$ under 365 nm UV light; (b) The fluorescence intensity of complex **1** in MnO_4^- solution as a function of exposure time. Inset: the color changes of complex **1** induced by the addition of 1.0 mM MnO_4^- under 365 nm UV light.

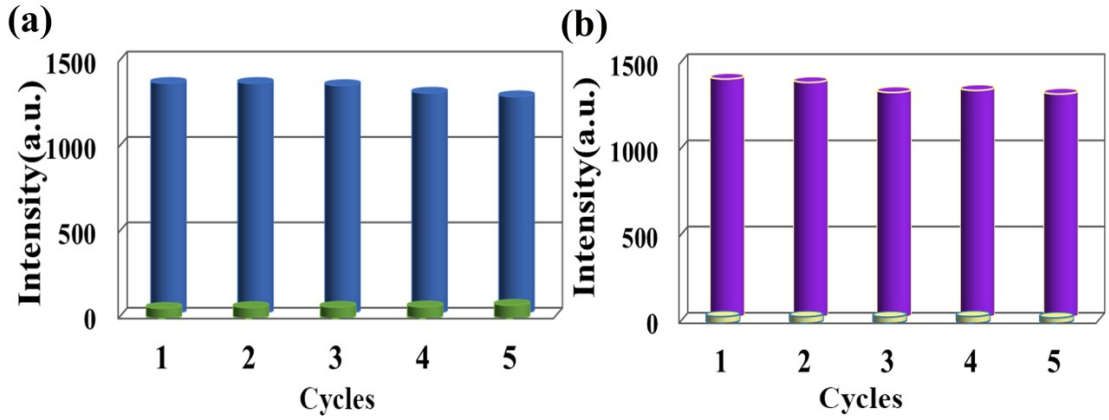

Fig. S16 (a) Photoluminescence intensity of complex **1** in five recyclable experiments for the $Cr_2O_7^{2-}$ in aqueous solution; (b) Photoluminescence intensity of complex **1** in five recyclable experiments for the MnO_4^- in aqueous solution.

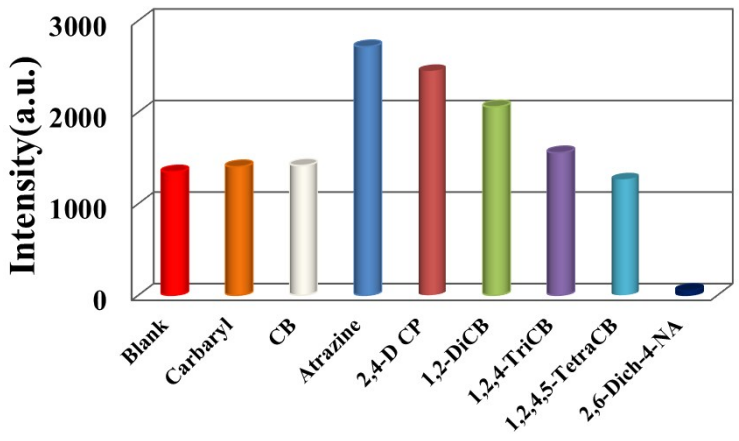

Fig. S17 Fluorescence intensity of complex **1** dispersed in various 0.01 M pesticides.

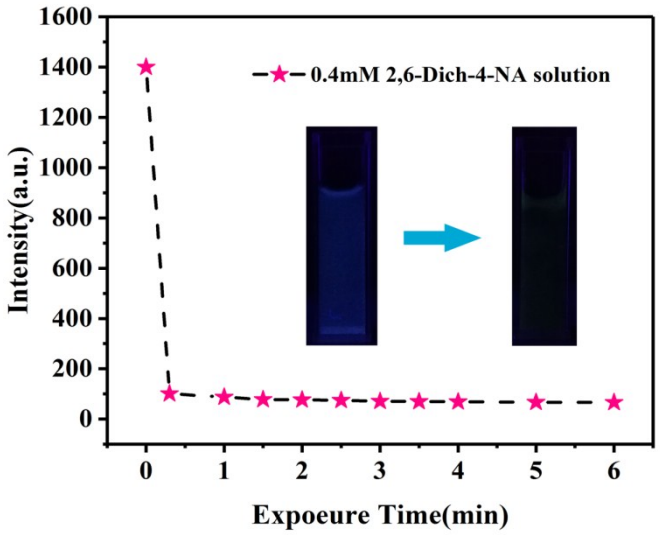

Fig. S18 The fluorescence intensity of complex **1** in 2,6-Dich-4-NA solutions as a function of exposure time. Inset: the color changes of complex **1** induced by the addition of 0.4 mM 2,6-Dich-4-NA under 365 nm UV light.

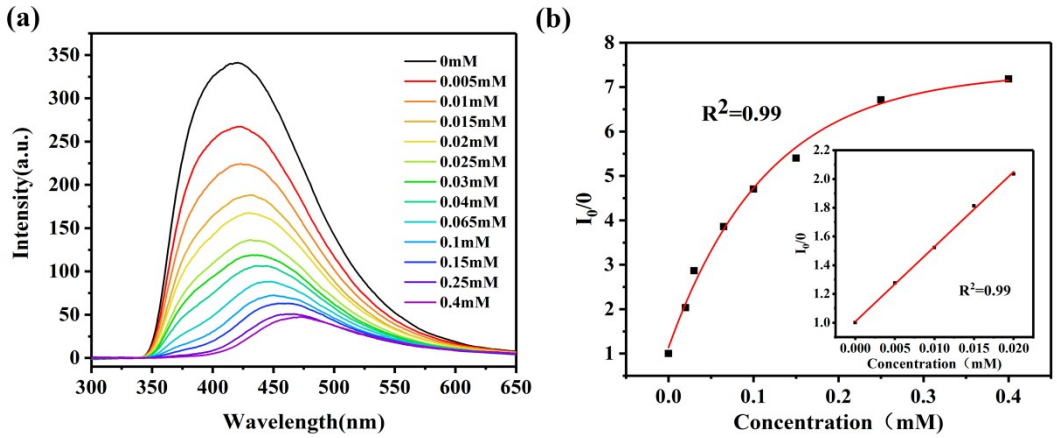

Fig. S19 (a) Fluorescence intensity of complex **1** for sensing of 2,6-Dich-4-NA dispersed in surfactant molecule in the medium. (b) SV plot of complex **1** for sensing of 2,6-Dich-4-NA in surfactant molecule in the medium. Inset: linear fitting part.

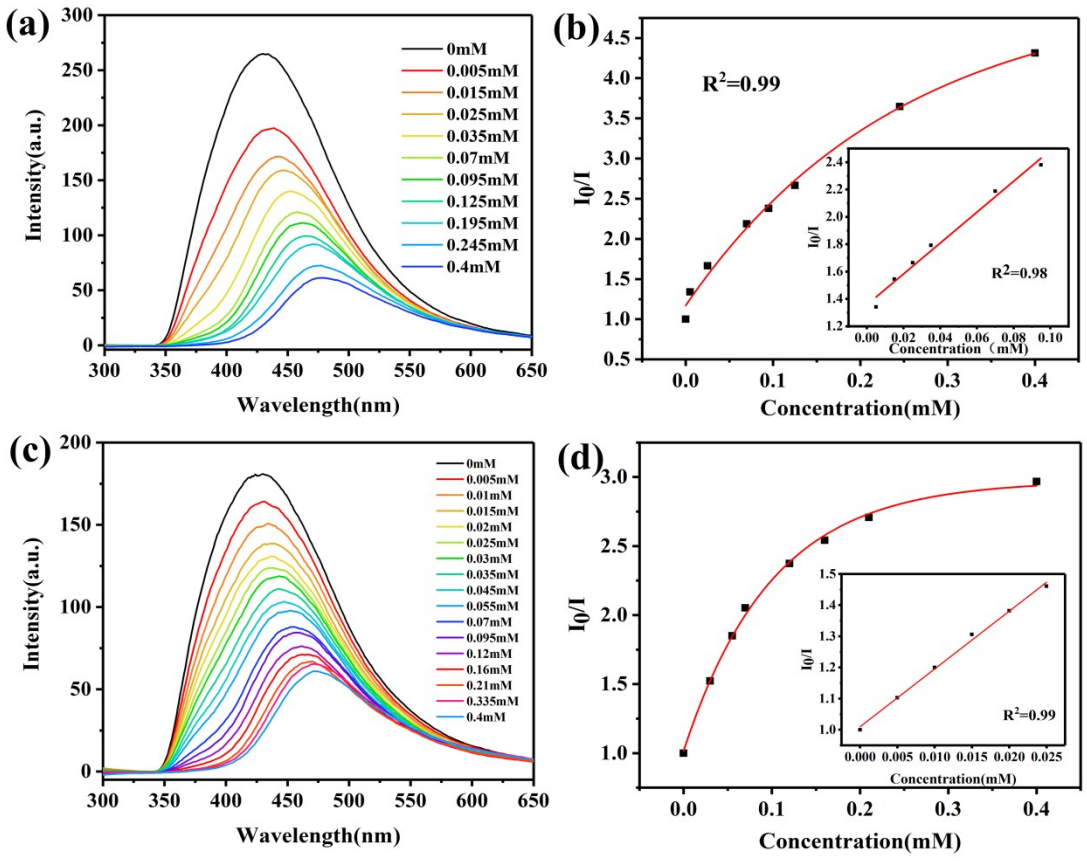

Fig. S20 The fluorescence spectra of complex **1** with different concentrations of 2,6-Dich-4-NA in aqueous solution including 100 μL nectarine extract (a) and grape extract (c). SV plot of complex **1** for sensing of 2,6-Dich-4-NA in aqueous solution including 100 μL nectarine extract (b) and grape extract (d). Inset: linear fitting part.

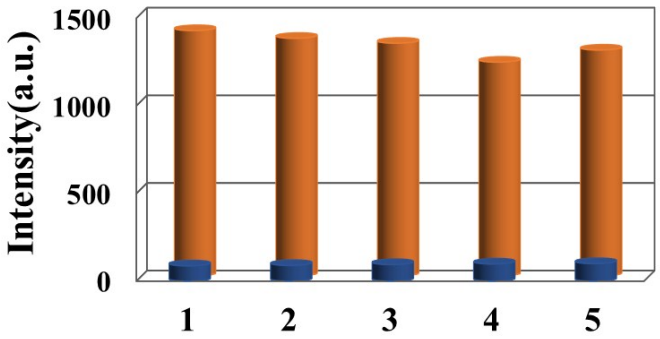

Fig. S21 Photoluminescence intensity of complex **1** in five recyclable experiments for the 2,6-Dich-4-NA in aqueous solution.

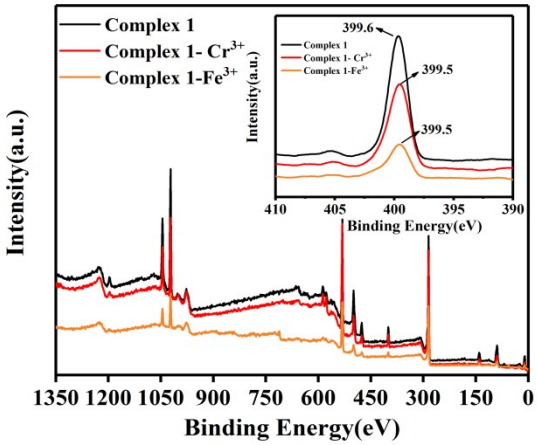

Fig. S22 XPS spectra of complex **1**, complex **1**-Fe^{3+} and complex **1**-Cr^{3+}. Inset: XPS spectra of N1s for complex **1**, complex **1**-Fe^{3+} and complex **1**-Cr^{3+}.

References

1 (a) D. K. Singha, P. Majee, S. Mandal, S. K. Mondal, and P. Mahata, *Inorg. Chem.*, 2018, **57**, 12155-12165;

(b) D. K. Singha, P. Majee, S. K. Mondal and P. Mahata, *ChemistrySelect.*, 2017, **2**, 5760-5768.